



Bisphenol A attenuation in natural microcosm: Contribution of ecological components and identification of transformation pathways through stable isotope tracing



Yan Li^{a,b}, Han Zhang^a, Azhar Rashid^{a,c}, Anyi Hu^a, Kuikui Xin^e, Haoran Li^e, Bob Adyari^{a,b}, Yuwen Wang^{a,b}, Chang-Ping Yu^{a,d}, Qian Sun^{a,*}

^a CAS Key Laboratory of Urban Pollutant Conversion, Institute of Urban Environment, Chinese Academy of Sciences, Xiamen, Fujian 361021, China

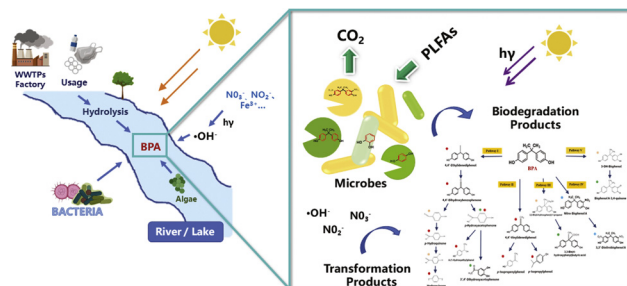
^b University of Chinese Academy of Sciences, Beijing 100049, China

^c Nuclear Institute for Food and Agriculture, Tarnab, Peshawar 25000, Pakistan

^d Graduate Institute of Environmental Engineering, National Taiwan University, Taipei 106, Taiwan

^e College of Environment and Ecology, Xiamen University, Xiamen, Fujian 361005, China

GRAPHICAL ABSTRACT



ARTICLE INFO

Editor: Deyi Hou

Keywords:

BPA

Natural attenuation

Transformation products

GC-C-IRMS

Path coefficient analysis

ABSTRACT

Residues of bisphenol A (BPA) are ubiquitously detected in the surface water due to its widespread usage. This study systematically investigated the dissipation and kinetics of BPA under simulated hydrolysis, direct and indirect photolysis, bacterial degradation, microbial degradation and natural attenuation in microcosm. Structural equation modeling (SEM) by using partial least square method in path coefficient analysis suggested that the microbial degradation was the major factor involved in the natural attenuation of BPA. The potential transformation products were identified by using liquid chromatography high-resolution mass spectrometry (LC-HRMS) and stable isotope tracing technique by simultaneous performing gas chromatography combustion isotope ratio mass spectrometry (GC-C-IRMS) and gas chromatography mass spectrometry (GC-MS). A total of fourteen including three novel transformation products of BPA were identified to indicate five possible pathways. An increased yield of labeled ($\delta^{13}\text{C}$) CO_2 and detection of ^{13}C -labeled phospholipid fatty acids (PLFAs) indicated the mineralization of BPA and possible utilization of BPA or its transformation products by microbes for cellular membrane synthesis, respectively.

* Corresponding author.

E-mail address: qsun@iue.ac.cn (Q. Sun).

<https://doi.org/10.1016/j.jhazmat.2019.121584>

Received 26 August 2019; Received in revised form 18 October 2019; Accepted 31 October 2019

Available online 04 November 2019

0304-3894/ © 2019 Elsevier B.V. All rights reserved.

1. Introduction

Bisphenol A (2,2-bis (4-hydroxyphenyl) propane, BPA) is used in the manufacturing of epoxy resins and polycarbonate plastics, which is primarily applied to the production of plastic consumer products (Vandenberg et al., 2007). Due to the extensive usage and release as monomers, BPA is widely detected in various types of environmental media in different parts of the world. BPA residues were detected in the surface water of rivers and estuaries at concentrations ranging between 10.6–364 ng L⁻¹ in China (Liu et al., 2017; Sun et al., 2016; Zhao et al., 2019); 6.5–431 ng L⁻¹, 4.6–272 ng L⁻¹, 54–1950 ng L⁻¹ in Japan, Korea and India, respectively (Yamazaki et al., 2015), while, the freshwater concentrations of BPA ranged between 5–300 ng L⁻¹ in Europe and North America (Staples et al., 2018). BPA is an endocrine disrupting chemical (EDC) and has been found to cause cellular toxicity, reproductive disorders, and neurotoxicity in human being and other living organisms at sub-lethal concentrations (Chen et al., 2016; Yan et al., 2017; Zhao et al., 2019). Therefore, an understanding of the environmental fate of BPA in the surface water is needed.

In the natural aquatic environment, BPA can attenuate in different possible ways. Bio-degradation by the secretions (Eio et al., 2015; Zhang et al., 2013) or enzyme (Ji et al., 2018; Yu et al., 2018) from bacteria or fungi is reported. In some other studies, the photo-degradation was reported as the major pathway for the natural attenuation of BPA in the surface water (Neamtu and Frimmel, 2006; Peng et al., 2006), where, between the photo-degradation processes, the indirect photo-degradation that involves generation of reactive oxygenated species by the organic matter content was proved to be more efficient than the direct photo-degradation to attenuate BPA (Barbieri et al., 2008). In addition, the role of hydrolysis has also been reported in the natural attenuation of BPA (Hou et al., 2017; Sun et al., 2012). Despite that many environmental factors have been found to contribute to the natural attenuation of BPA, yet, almost all the previous studies focused on the role of single factor in isolation (Barbieri et al., 2008; Peng et al., 2006; Yang et al., 2020). Contribution of many factors clearly indicates that the attenuation of BPA under natural aquatic conditions is a fairly complex phenomenon. However, the knowledge about the contribution of a variety of the biotic and abiotic factors and their possible interactions during the attenuation of BPA under natural aquatic environment is limited. Recently, a structural equation modeling (SEM) approach by employing partial least square technique in path coefficient analysis was successfully applied to elucidate the contributions of different biotic and abiotic environmental factors in the natural attenuation of sulfamethoxazole (Li et al., 2018). SEM was able to elucidate the direct and indirect contribution of different factors along with their statistical significance and effect sizes in the sulfamethoxazole attenuation (Li et al., 2018). A similar approach was also used in this study and the contribution and interactions of different environmental factors in the natural attenuation of BPA was investigated.

According to Fenner et al., degradation process may involve both biotic and abiotic processes, and the emerging transformation products are determined by the structural affinity of the pollutants to specific types of degradation pathway as well as to the environmental conditions it is exposed (Fenner et al., 2013). These processes have led to diverse types of transformation products and degradation intermediates of BPA, including 4-isopropenylphenol, 4-hydroxybenzaldehyde, 4-hydroxybenzoate, 4-hydroxyacetophenone, 4-hydroxycumyl alcohol, hydroquinone, BPA monomethyl ether, BPA dimethyl ether, 3-nitro-BPA, 3,3'-dinitro-BPA that involve oxidation, cleavage formation, methylation, and hydrolysis of parent compound in the aquatic environment (Im and Löffler, 2016; McCormick et al., 2011). Detection of transformation products essentially provide crucial evidence to understand the degradation pathways of BPA. So far, application of liquid chromatography coupled with mass spectrometry and especially, the high-resolution tandem mass spectrometry (HRMS) technique like

quadrupole/time of flight-mass spectrometry (Q/ToF-MS) has been used for the analysis the BPA transformation products. The mass spectrometry for the targeted analysis of the transformation products can be straightforward if the products are known. However, it can be challenging for the suspected or non-targeted screening of transformation products (Bletsou et al., 2015; Fenner et al., 2013). The challenges posed by coelution, identical mass spectra and low concentrations of metabolites has been successfully dealt with the use of stable isotope tracing coupled with HRMS in metabolomics (Tian et al., 2018). This additional data analysis strategy can also efficiently compensate the MS data volume limitations, the complexity of the environmental matrix, and low concentration or abundance of the micropollutants in complex matrices (Hofstetter and Berg, 2011) to provide an efficient way for the identification of hitherto unknown transformation products and underlying transformation mechanisms (Limam et al., 2016; Tian et al., 2018).

In this study, attenuation of BPA was investigated at a microcosm scale at environmental concentrations to mimic the natural environmental conditions of the surface water in a subtropical river. Therefore, special emphases were placed for: (1) the identification of potential transformation products by employing stable isotope tracing technique. This was achieved by using stable isotope labelled BPA and subsequently analysis by HRMS (LC-Q/ToF-MS), gas chromatography coupled with mass spectrometry (GC-MS); and combustion isotope ratio mass spectrometry (GC-C-IRMS), (2) understanding BPA attenuation kinetics under simulated hydrolysis, direct photolysis, indirect photolysis, bacterial degradation, microbial degradation and natural attenuation conditions, and (3) elucidating the contribution and interactions of environmental factors during the natural attenuation of BPA.

2. Materials and methods

2.1. Chemicals and reagents

Certified reference standards of BPA (99 % purity) and benzene ring ¹³C labeled BPA (Rings-¹³C₁₂, 99 % purity) were obtained from Sigma-Aldrich Inc. and Cambridge Isotope Laboratories Inc., respectively. The CAS numbers, molecular formula, molecular weight, and chemical structures of the standards are shown in Table S1 in the Supplementary information (SI). Methanol, *n*-hexane and acetone of HPLC grade were provided by Merck Inc. The derivatization reagents, pyridine (99.5 %) was obtained from Alfa Aesar; N,O-bis(trimethylsilyl)trifluoroacetamide (BSTFA) containing 1 % trimethylchlorosilane (TMCS) was purchased from Regis Technologies Inc.

2.2. Microcosm study of BPA dissipation

BPA dissipation in microcosm was simultaneously conducted in duplicate under six simulated conditions to mimic illuminated natural attenuation, bacterial degradation, microbial degradation, direct photo-degradation, indirect photo-degradation, and hydrolysis (Table S2 in SI). The microcosm constituted water sample (1.05 L) placed in glass beakers (3.0 L) with quartz lid. Surface water samples collected from Jiulong River (24.42155°N, 117.78783°E) were used in the natural attenuation, bacterial degradation and microbial degradation. An account of water quality parameters are given in Table S4. Autoclaved surface water (121 °C, 100 kPa, 20 min.) was used in the hydrolysis and indirect photo-degradation, while Milli-Q water was used in the direct photo-degradation study. In the case of bacterial degradation, the surface water samples were filtered through 2 μm mixed cellulose membrane filters to exclude the phytoplankton and zooplankton and to facilitate the bacterial microflora (Chen et al., 2015). The natural attenuation, direct and indirect photo-degradation were conducted under natural sunlight, while, the bacterial degradation and hydrolysis treatments were kept in dark with aluminum foil wrapping to avoid exposure to light. The microbial degradation was studied under red ($\lambda = 635$ nm)

monochromatic visible light (15 W, Sanyi Lighting Electronics Co. Ltd) to exclude the effect of photolysis and to facilitate the algal growth (Jasper et al., 2014). The sunlight intensity was monitored in real-time by HOBO onset pendant (UA-002, HOBO, USA) as shown in SI Fig. S1. In view of the environmental concentrations of BPA, the water samples for the six simulated conditions were spiked to achieve $5.0 \mu\text{g L}^{-1}$ initial BPA concentration (Yang et al., 2014). Both, dissolved and volatilized BPA transformation products were monitored in setting separate experiments by using stable carbon isotope labelled $^{13}\text{C}_{12}$ -BPA. For the dissolved BPA transformation products, a separate of natural attenuation microcosm was conducted, where, $^{13}\text{C}_{12}$ -BPA and BPA were used in mix at 0.05 mg L^{-1} and 0.45 mg L^{-1} concentrations, respectively. Furthermore, volatilized BPA transformation products were studied in yet another natural microcosm spiked with $^{13}\text{C}_{12}$ -BPA at an initial concentration of 0.5 mg L^{-1} . Headspace air samples were collected for the volatilized BPA transformation products resulting from BPA mineralization.

2.3. Quantitative analysis of BPA dissipation and water parameters

Aliquot (1.0 mL) of water samples were collected at 0, 8, 24, 48, 96, 168 h intervals, filtered through PTFE membrane filters ($0.2 \mu\text{m}$, 17 mm, Anpel laboratory technologies Inc., Shanghai) and stored in amber vials (9 mm, Anpel laboratory technologies Inc., Shanghai) at 4°C to prevent further transformation. The BPA concentrations together with the two potential transformation products (nitro-BPA and dinitro-BPA) were determined with high performance liquid chromatography (HPLC, Shimadzu LC-20A, Japan) electrospray ion sources with triple quadrupole mass spectrometer (ESI-MS/MS, Applied Biosystems ABI 6500, USA) in negative ionization mode. Chromatographic separation was achieved by C18 column (Kinetex C18, $2.6 \mu\text{m}$, $100 \times 2.1 \text{ mm}$; Phenomenex) at flow rate of 0.3 mL/min for mobile phases A (5 mM ammonium acetate in Milli-Q water) and B (methanol) in a gradient program as shown in Table S3 (Sun et al., 2012). BPA was quantified against reference standard calibration regimes, while, only signal intensities were recorded for nitro-BPA and dinitro-BPA. Method detection limits (MDLs) for BPA was 73.5 ng L^{-1} .

The quality parameters of Jiulong River surface water viz, total organic carbon (TOC), total nitrogen (TN), total carbon (TC) and inorganic nitrogen (IN) were analyzed by the total organic carbon analyzer (TOC-VWP, Shimadzu, Japan). The pH was measured by Multi 3430 set G (WTW, Germany). The dissolved total nitrogen (DTN), nitrate-nitrogen ($\text{NO}_3\text{-N}$), nitrite-nitrogen ($\text{NO}_2\text{-N}$), ammonium-nitrogen ($\text{NH}_4\text{-N}$), dissolved reactive phosphorus (DRP) and dissolved total phosphorus (DTP) were measured by continuous flow injection (AA3, SEAL Analytical GmbH, Norderstedt, Germany). The values of the water quality parameter are given in Table S4.

2.4. Identification of transformation products

2.4.1. GC-MS and GC-C-IRMS

GC-MS (6890 series GC coupled with 5975C series quadrupole MS, Agilent, Palo Alto, CA) and GC-C-IRMS (Delta V advantage, Thermo Fisher Scientific, USA) techniques were used in parallel for the initial screening and stable isotope base confirmation of the transformation products, respectively. In order to achieve similar retention times in both the techniques, same column (Agilent HP-5 GC-MS, $30 \text{ m} \times 0.32 \text{ mm}$, $0.25 \mu\text{m}$) and temperature programs were used. Similar retention times helped to locate the potential transformation products based on the specific response ($m/z = 45$) in both the techniques. The GC conditions are shown in Text S1.

Aliquot (50 mL) of water samples were collected from the natural attenuation batch spiked with $^{13}\text{C}_{12}$ -BPA at 0, 24, 48, 96, and 168 h intervals. Samples were concentrated by solid phase extraction (SPE) using Oasis HLB cartridges (500 mg, 6 mL, Waters) followed the method reported by Sun et al. (2016). The enriched samples were derivatization

according to the method reported by Ma et al. (2016) and analysis by GC-MS and GC-C-IRMS in parallel for screening and confirmation of stable isotope labeled transformation products. GC-C-IRMS was used for stable carbon isotopic tracing to detect the mass of CO_2 in terms of 44, 45 and $46 m/z$, where, the chromatographic peak of $45 m/z$ indicated the potential ^{13}C -labeled transformation products of $^{13}\text{C}_{12}$ -BPA. Later, the GC-MS was used in full scan mode with the range of $30\text{--}600 m/z$ to identify the chemical structure of the $^{13}\text{C}_{12}$ -labeled transformation products. The structures of the candidate transformation products was identified and picked by the GC-C-IRMS technology. Meanwhile, the structures were further confirmed by manually comparing the full-scan GC-MS spectra with the standard spectra of National Institute of Standards and Technology (U.S. Department of commerce NIST chemistry webbook, SRD 69) and Spectral Database for Organic Compounds (SDBS). In addition, the headspace air samples were collected to monitor $^{13}\text{C}_{12}$ -BPA mineralization into carbon isotope labeled volatile transformation products by GC-C-IRMS.

2.4.2. LC-Q/ToF-MS

The enriched time interval samples were also analyzed by LC-Q/ToF-MS (Q-TOF, H-Class-Xevo G2-S, Waters, Guyancourt, France) in negative ESI mode with data collection by MS^E methodology. LC gradient program is shown in Table S5. Simultaneous acquisition of the parent ion and subsequent fragmentation by both MS and MS/MS functions were achieved by using 0.2 s scan time and 14 ms inter-scan delay. The capillary voltages and lockspray capillary were set at 2.5 kV and 1.20 kV, dissolution and source temperature were set at 450°C and 120°C , respectively, and cone gas was applied at a flow rate of 50 L h^{-1} . The injection volume was $5.0 \mu\text{L}$ and the mass accuracy was maintained by using a lockspray function with leucine-enkephalin. MS was conducted with low collision energy (-6 V) scan with mass range from 50 to $750 m/z$, while, MS/MS was conducted at higher ramped range from -10 to -45 V to induce fragmentation mass range from 50 to $750 m/z$. All data collection was performed in sensitivity mode (Resolution = $30,000\text{--}40,000$). The identification of the transformation products was carried out by the suspect screening as proposed by Helbling et al. (2010) and Bletsou et al. (2015). In the suspect screening, candidates were proposed on the basis of University of Minnesota Pathway Prediction System (UM-PPS) (Gao et al., 2010) with subsequent screening and confirmation by using MetaboLynx XS v4.1 (Waters, Milford, USA) software with an accepted mass accuracy of 5 ppm (Brenton and Godfrey, 2010).

2.5. Microbial community characterization

FastDNA SPIN kit for soil (Qbiogene-MP Biomedicals, Irvine, CA, USA) was used for the DNA extraction. Total DNA was extracted from 4 samples (Day 0, Day 7 NA, Day 7 DM, Day 7 MD) using the modified protocol established by Hu et al. (Hu et al., 2014). A 16S rRNA gene amplicon sequencing was made from field sample using universal primers (515F and 907R), and 16S DNA sequencing was carried out by using Illumina MiSeq (Illumina Inc., San Diego, CA, USA) by Beijing Novogene Bioinformatics Technology.

2.6. Statistical analysis

2.6.1. Degradation kinetics

BPA underwent degradation following the pseudo-first-order kinetic model, as shown in Eq. (1):

$$-\ln(C_t \times C_0^{-1}) = k \times t \quad (1)$$

where, C_0 and C_t are the BPA concentrations at the initial and at any time "t", respectively. The transformation rate constant (k) and half-lives (T_{50}) were calculated by Eqs. (2) and (3), respectively.

$$k = -\ln(C_t \times C_0^{-1}) \times t^{-1} \quad (2)$$

$$T_{50} = \ln(2) \times k^{-1} \quad (3)$$

2.6.2. Coefficient effect analysis

Path coefficient analysis was used to describe the contribution of different biotic and abiotic factors in the natural attenuation of BPA by following Li et al. (2018). Path coefficient analysis was used through SEM approach by employing partial least square multiple regressions to understand the contribution of illuminated natural attenuation, bacterial degradation, microbial degradation, direct photo-degradation, indirect photo-degradation, and hydrolysis in the natural attenuation of BPA. SEM analysis was systematically performed through specifying and evaluating model, parameter evaluation for direct and indirect contributions and overall goodness of fit by WarpPLS (Version 6.0, USA). Appropriateness of the model was evaluated based on ten global model fit and quality indices entailed in Table S6. The *p*-values give the level of significance of path coefficients, and the relative importance of each variable is described as effect size (ES) of each path coefficient, where, the values of ES viz. 0.02, 0.02, 0.15, and 0.35 indicate too weak, small, medium, and large effect size, respectively. In addition, the correlation between BPA dissipation rate and environmental factors viz. DIN, ammonia, nitrite, nitrate, TOC, TC, and TN was performed by using R studio software (v1.1.463, Inc., Boston, USA).

3. Results and discussion

3.1. BPA dissipation kinetics

The dissipation of BPA (C_t/C_0) under different simulated conditions in the microcosm study is shown in Fig. 1. The dissipation efficiency in the natural attenuation, indirect photo-degradation, hydrolysis, bacterial degradation and microbial degradation treatments reached 100 % within 168 h, however, scarce dissipation was observed in the direct photo-degradation. BPA dissipation followed the pseudo-first-order kinetic model. The kinetics models, goodness of fit (R^2), rate of degradation given as slope (k , h^{-1}), and half-lives (T_{50} , h) are shown in Table 1. The half-life values for natural attenuation, indirect photolysis, hydrolysis, bacterial degradation, microbial degradation were 25.7, 31.5, 33.0, 23.1 and 25.7 h, respectively, while, the calculation of half-life for the direct photolysis was not feasible.

Spearman's unadjusted correlation studied the relationship between BPA dissipation and the water parameters. Results showed a strong correlation ($r = 0.93$) of BPA dissipation with TC, TOC and ammonia at a 95 % level of significance ($p = 0.05$) as shown in Fig. S2a. In the aquatic environment, carbon and nitrogen may serve as nutritional sources for the microbial growth and community variation (Subagio

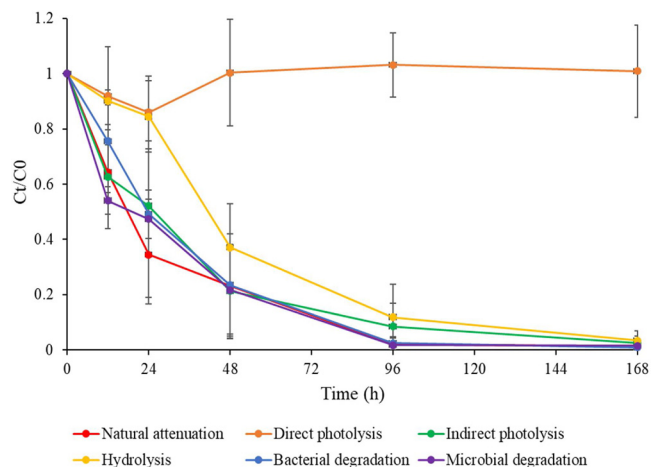


Fig. 1. BPA dissipation in surface water samples (error bars indicate \pm standard error of mean).

Table 1

Kinetic equations, goodness of fit (R^2), slope (k , h^{-1}), and half-lives (T_{50} , h) of BPA dissipation.

	Degradation kinetic equation	R^2	Degradation kinetics (k , h^{-1})	T_{50} (h)
Natural attenuation	$y = 0.7467e^{-0.027x}$	0.9130	0.0270	25.7
Direct photolysis	$y = 0.9224e^{-1e^{-04x}}$	0.0004	/	/
Indirect photolysis	$y = 0.8082e^{-0.022x}$	0.9792	0.0220	31.5
Hydrolysis	$y = 1.1113e^{-0.021x}$	0.9868	0.0210	33.0
Bacterial degradation	$y = 0.9215e^{-0.03x}$	0.9555	0.0300	23.1
Microbial degradation	$y = 0.7496e^{-0.027x}$	0.8924	0.0270	25.7

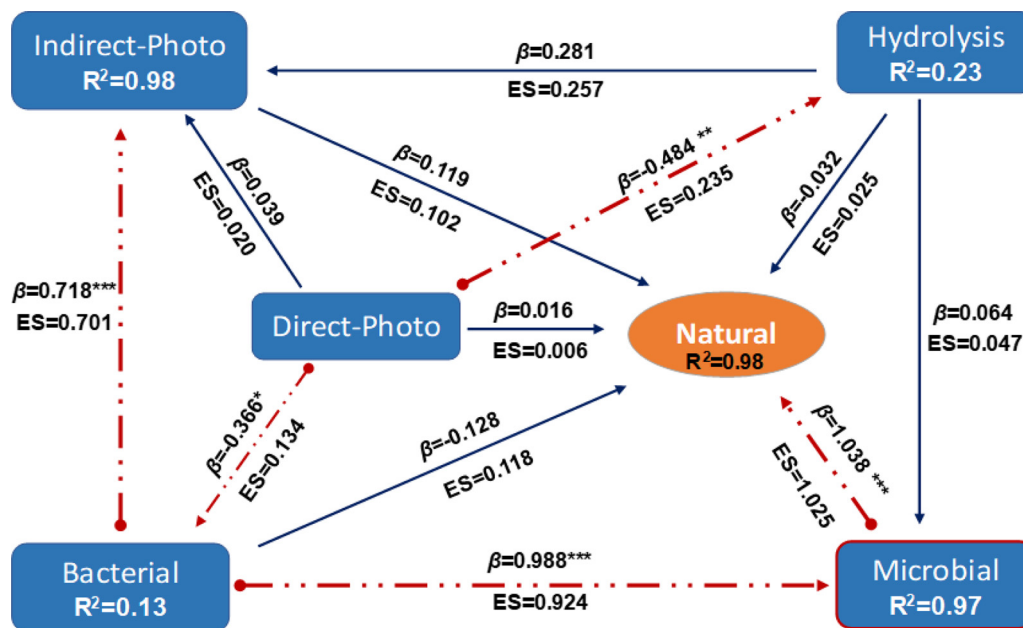
/, not evaluated.

et al., 2010), and consequently resulted in the bacterial or microbial degradation of BPA (Luo et al., 2019). The dissolved carbon and nitrogen can also contribute to photosensitized oxidation or chemical oxidation (Ding et al., 2016; Yang et al., 2018; Zielinska et al., 2014) to cause BPA dissipation via indirect photolysis and hydrolysis. A significantly negative correlation was observed between the BPA dissipation and nitrite concentrations in the hydrolysis group as shown in Fig. S2 (d). Previous studies suggested that the abiotic nitrification between nitrite and phenolic compounds including BPA (Sun et al., 2012), which indicated that nitrite played a vital role in the BPA dissipation in the hydrolysis microcosm set.

3.2. Path coefficient analysis

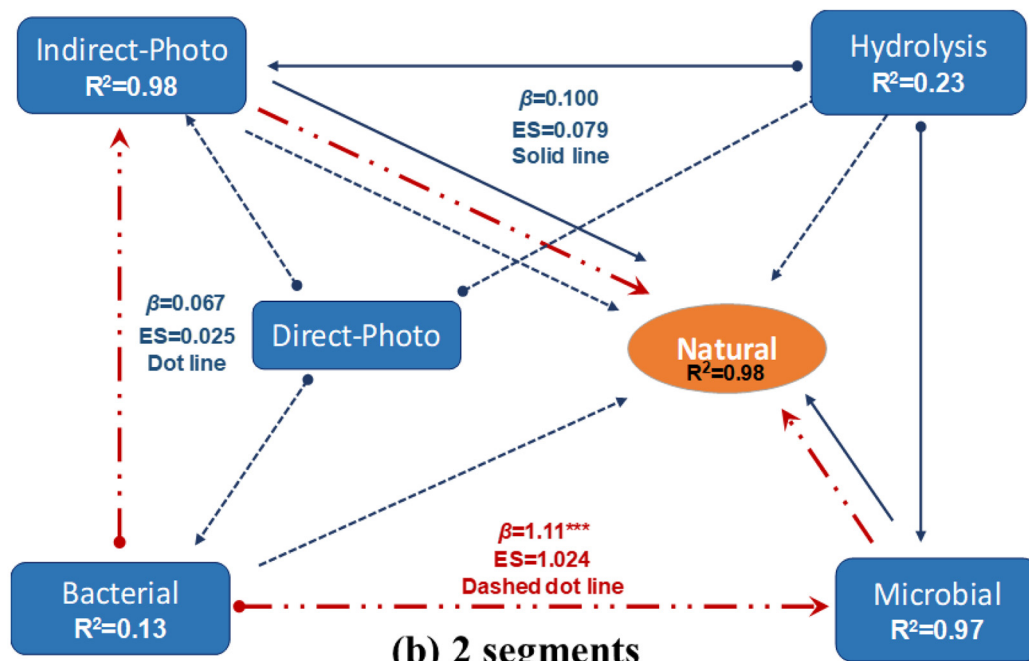
SEM was conducted to evaluate the contribution of different biotic and abiotic environmental factors on the natural attenuation of BPA. The goodness of fit and other quality indices, given in Table S6, indicated the appropriateness of the proposed SEM. The β -values indicate the path coefficients along with the level of significance as *p*-values, and the effect sizes (ES) indicate the relative importance of the effect of the independent variable on a dependent variable Fig. 2a. The model explained 98 % ($R^2 = 0.98$) variability in the natural attenuation as a dependent variable under the influence of sole effects of direct photolysis, indirect photolysis, hydrolysis, microbial degradation and bacterial degradation. The model presents 12 direct effects of the independent variable on the dependent variables. The results suggested that the microbial degradation was the only major factor with highly significant ($p < 0.001$) direct contribution on the natural attenuation of BPA with a medium effect size of $ES = 1.025$. The other four factors viz. direct photolysis, indirect photolysis, hydrolysis, microbial degradation and bacterial degradation did not show significant effect on the natural attenuation of BPA. Bacterial degradation showed significant relation with microbial degradation ($\beta = 0.988$, $p < 0.001$) and indirect photolysis ($\beta = 0.718$, $p < 0.001$) with nearly medium effect sizes of 0.92 and 0.71, respectively. The SEM model explained fairly high variability ($R^2 \sim 0.97$) for bacterial degradation with microbial degradation and indirect photolysis as response variables. However, a statistically significant direct effect of direct photolysis on hydrolysis and bacterial degradation were deemed unimportant due to very low explained variability (23 % and 13 %, respectively) of the response variables. The present results are consistent with the previous findings, where, the bacteria and other microbes were the predominant factors responsible for the dissipation of BPA in the aquatic environment (Zhang et al., 2013). BPA was found un-degradable by the direct exposure to visible light; however, it underwent degradation by the exposure to UV light in the aqueous solution (Barbieri, Massad et al. 2008). Furthermore, the direct photolysis pathway of BPA degradation was also concluded inconsequential, due to the screening effects in natural waters (Barbieri et al., 2008; Chin et al., 2004).

SEM was also helpful in explaining the mediatory role of biotic and



(a) 1 segment

..... Significant ——— Non significant



(b) 2 segments

..... The path coefficient start from bacterial to natural attenuation (Significant)
 ——— The path coefficient start from hydrolysis to natural attenuation (Non significant)
 - - - - - The path coefficient start from direct-photo to natural attenuation (Non significant)

Fig. 2. Hypothetical SEM: (a), one segment; (b), two segments. The directions of the arrows represent the hypothesized relationships between the variables. R^2 is the coefficient of determination indicating the variability explained for each dependent variable. β -values indicate the path coefficients. The level of significance correlation is indicated by $^*(p < 0.05)$, $^{**}(p < 0.01)$, and $^{***}(p < 0.001)$. The impact of an independent variable on a dependent variable is given by $ES < 0.02$ (too weak), > 0.02 (small effect), > 0.15 (medium effect) and > 0.35 (large effect).

abiotic components in the natural attenuation of BPA. Among the two-segment indirect effects (Fig. 2b), bacterial degradation had a highly significant effect ($p < 0.001$) on the natural attenuation of BPA, through the mediation of indirect photolysis and the microbial degradation with medium size effect ($ES = 1.02$) (Fig. 2b & Table S7). The microbial degradation may involve other microbes like algae beside bacteria in the BPA attenuation. The role of indirect photo-degradation was also put forward in BPA dissipation in a previous study (Peng et al., 2006). The facilitation of bacterial degradation might be due to the readily biodegradable transformation products from the indirect photo-degradation (Vione et al., 2014; Yu et al., 2018). In addition, the metabolic intermediates from bacteria might also facilitate the indirect photolysis.

3.3. BPA degradation

3.3.1. Identification of transformation products

Identification of the BPA transformation products was carried out by GC-C-IRMS and GC-MS techniques. GC-C-IRMS combusts the separated organic compounds and releases CO_2 as a transformation product. Measurement of the isotopic CO_2 by mass spectrometry provides information about the possible BPA transformation products. The chromatogram produced by GC-C-IRMS is shown in Fig. 3a, where, m/z 44, 45 and 46 indicate the ions of $^{12}\text{C}^{16}\text{O}_2$, $^{13}\text{C}^{16}\text{O}_2$, and $^{13}\text{C}^{16}\text{O}^{17}\text{O}$, respectively. With the specific tracer ^{13}C -isotope, parent BPA (Peak 6) and its nine potential transformation products can be clearly recognized in terms of m/z 45 (Fig. 3a). To measure the m/z of the identified ^{13}C -isotope peaks in GC-C-IRMS analysis, GC-MS was used with the same GC column and temperature program and the m/z of the eluting transformation products was measured. GC-MS chromatogram of $^{13}\text{C}_{12}$ -BPA and its nine potential transformation products is shown in Fig. 3b. The m/z data was then used to elucidate the molecular structure of each transformation product by comparing with the NIST database as shown in Table S8. During this study, three novel transformation products of BPA viz. 4,4'-vinylidenediphenol, 4,4'-ethylidenediphenol, and 4,4'-dihydroxybenzophenone were identified. To the best of our knowledge, these three BPA transformation products are identified for the first

time. The transformation products identified by the use of stable isotope tracing technique were *p*-isopropenylphenol (Peak 1), hydroquinone (Peak 2), *p*-hydroxyacetophenone (Peak 3), *p*-hydroquinone (Peak 4), 4-(1-hydroxyethyl)phenol (Peak 5), 4,4'-vinylidenediphenol (Peak 7), *p*-isopropylphenol (Peak 8), 4,4'-ethylidenediphenol (Peak 9), and 4,4'-dihydroxybenzophenone (Peak 10) (Fig. 3b). These transformation products indicate demethylation, oxidation and skeletal rearrangement pathways for BPA attenuation. The major advantage of the proposed GC-C-IRMS method was its high selectivity and sensitivity to identify the parent BPA at low concentration and its ability to track down unknown transformation products at even lower concentrations in the complex matrix.

Considering the limitations of poor volatility, high polarity, or thermo-instability of some intermediates in GC analysis, the LC-Q/ToF-MS was used to characterize the potential intermediates (Agüera et al., 2013). Using suspect screening approach in LC-Q/ToF-MS analysis, five transformation products viz. *p*-hydroxyacetophenone, 3-nitro-BPA, 3',4'-dihydroxyacetophenone, BPA-3,4-quinone, and 3,3-bis(4-hydroxyphenyl) butyric acid were identified (Table 2). Their MS spectra were confirmed based on the isotope pattern of labelled stable carbon isotope.

3.3.2. Degradation pathways

Overall, fourteen transformation products were identified in this study. Five major pathways of BPA attenuation are proposed as shown in Fig. 4. In the pathway-I, demethylation of BPA yields 4,4'-ethylidenediphenol that further transforms as 4,4'-dihydroxybenzophenone via oxidative skeletal rearrangement. Subsequently, 4,4'-dihydroxybenzophenone can transform into *p*-hydroxyacetophenone and/or *p*-hydroquinone via C-C bond cleavage formation. The *p*-hydroxyacetophenone may transform into 3',4'-dihydroxyacetophenone and/or 4-(1-hydroxyethyl) phenol, while, *p*-hydroquinone further transform into hydroquinone. The variations on the peak areas of BPA transformation products by GC-C-IRMS verified the generation and further transformation of intermediates (Fig. S3). The similar pathway was also observed in the case of photo-fenton-like treatment of BPA to yield 4,4'-hydroxybenzophenone (Molkenthin et al., 2013) and the photocatalysis

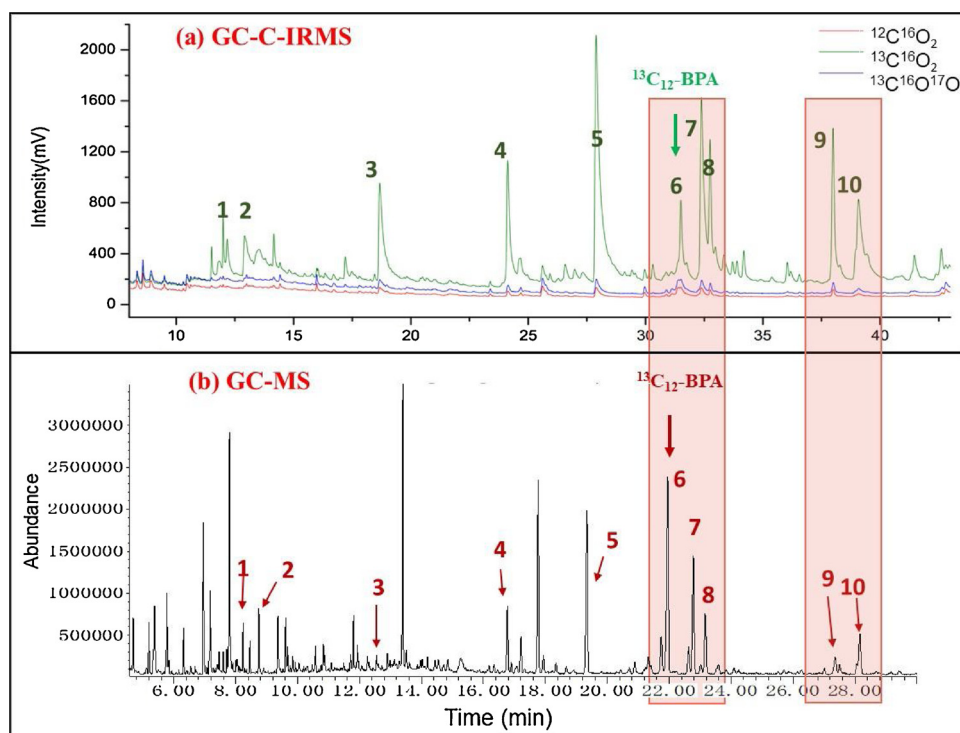


Fig. 3. Comparison of GC-C-IRMS (a) and GC-MS (b) chromatograms. (1) *p*-Isopropenylphenol; (2) hydroquinone; (3) *p*-hydroxyacetophenone; (4) *p*-hydroquinone; (5) 4-(1-hydroxyethyl)phenol; (6) bisphenol A; (7) 4,4'-vinylidenediphenol; (8) *p*-isopropylphenol; (9) 4,4'-dihydroxybenzophenone and (10) 4,4'-ethylidenediphenol.

Table 2
Five candidate transformation products detected based on the suspected screening approach.

Candidates name	Experiment condition	Mass m/z	Formula	Retention time(min)	Calculated mass (m/z)	Observed mass (m/z)	Error(ppm)	Proposed structure
p-Hydroxyacetophenone	Natural attenuation	136.0524	$C_8H_6O_2$	4.59	135.0441	135.0443	-2.4	
	Indirect photolysis			4.59		135.0443	-2.4	
	Hydrolysis			4.59		135.0442	-3.2	
	Microbial degradation			4.59		135.0445	-1	
	Bacterial degradation			4.59		135.0445	-1	
3',4'-dihydroxyacetophenone	Natural attenuation	152.0473	$C_8H_6O_3$	5.69	151.0390	151.0390	-3.6	
	Indirect photolysis			5.69		151.0389	-4.2	
	Hydrolysis			5.69		151.0394	-0.9	
	Microbial degradation			5.70		151.0391	-2.9	
	Bacterial degradation			5.69		151.0390	-3.6	
Nitro-bisphenol A	Natural attenuation	273.1001	$C_{15}H_{15}NO_4$	8.77	272.0917	272.0924	0.3	
	Indirect photolysis			8.77		272.0919	-1.5	
	Hydrolysis			8.77		272.0919	-1.5	
	Microbial degradation			8.77		272.0925	0.7	
	Bacterial degradation			8.75		272.0911	-4.4	
Bisphenol A-3,4-quinone	Microbial degradation	242.0943	$C_{15}H_{14}O_3$	8.00	241.0859	241.0861	-1.6	
	Microbial degradation			7.38		257.0808	-3.5	

degradation of BPA to 4-isopropenylphenol (Ju et al., 2018). Detection of 3',4'-dihydroxyacetophenone in water samples from natural attenuation, indirect photolysis, hydrolysis, bacterial and microbial degradation microcosm (Table 2), indicate that more than one environmental factor may be involved in this pathway.

In pathway-II, dehydrogenation of BPA yields 4,4'-vinylidenediphenol that further transforms to *p*-isopropenylphenol and/or *p*-isopropylphenol via cleavage reaction. In an earlier study, transformation of carbocationic isopropylphenol through the loss of H^+ and gain of H^- into *p*-isopropenylphenol and *p*-isopropylphenol was reported by using *Sphingomonas* sp. strain TTNP3 (Kolvenbach et al., 2007). The transformation products from pathway-II were detected from natural microcosm spiked with ^{13}C -labeled BPA (Table S8). In pathway-III, BPA hydrolysis yielded 2,2-bis(4-hydroxyphenyl)-1-propanol followed by 3,3-bis(4-hydroxyphenyl) butyric acid via oxidization. 3,3-bis(4-hydroxyphenyl) butyric acid was detected from microbial degradation microcosm in this study (Table 2). Lobos et al. also reported 2,2-bis(4-hydroxyphenyl)-1-propanol as BPA intermediate originating from *Sphingomonas* sp. strain MV1 treatment (Lobos et al., 1992). Pathway-IV involved nitration of BPA to nitro-BPA and dinitro-BPA. Both nitro- and dinitro-BPA were quantified using the LC-MS/MS. Intensities of nitro- and dinitro-BPA in different microcosm are plotted against time in Fig. S4. Nitro-BPA was detected at very early hours in natural microcosm and tended to remain constant until 48 h, and declined afterwards. In contrary, dinitro-BPA was barely detected until 48 h in the natural microcosm. However, an exponential increase of dinitro-BPA intensity was observed in the indirect photolysis after a lag phase of 24–48 h. Vione et al. reported the formation of dinitro-BPA as a consequence BPA nitration by $\cdot NO_2$ and $\cdot OH$ radicals (Eq. (4)) (Vione et al., 2014). This worth-mentioning here that 3-nitro-BPA was detected in all microcosm type in this study except direct photolysis (Table 2). In pathway-V, the hydroxylation of BPA (3-OH-bisphenol) and subsequently by the loss of H^+ , transforms into bisphenol A-3,4-quinone. Bisphenol A-3,4-quinone was detected in the microbial microcosm (Table 2). The genotoxicity of bisphenol A-3,4-quinone and its environmental implication were reported elsewhere (Kolsek et al., 2012).



The toxicity of BPA and its transformation products were estimated in terms of 50 % lethal concentration (LC_{50}) and chronic value (ChV) for fish, *Daphnid* and green algae by ECOSAR (v2.0) software program (Table S9). In the pathway I and III, the aquatic toxicity of the transformation products was generally lower than BPA. However, the aquatic toxicity of most transformation products in the pathway II, IV and V was higher than BPA, indicating the potential environmental risk raised by BPA natural attenuation.

Mineralization of BPA was investigated by quantifying $\delta^{13}C$ value of CO_2 in the headspace air samples from natural attenuation microcosm. The $\delta^{13}C$ value increased from -27.08% to 297.43% of the Vienna Pee Dee Belemnite (VPDB) international standard taken as a baseline after 96 h of incubation in the natural microcosm (Fig. S5). The increased values of $\delta^{13}C$ indicated the mineralization of $^{13}C_{12}$ -BPA to $^{13}CO_2$.

Moreover, lipid extraction and phospholipid fatty acid (PLFAs) analysis was performed according to the method reported by Wang et al. (2016). PLFAs are the cell membrane components of bacteria and other microbes. The mineralization and possible utilization of $^{13}C_{12}$ -BPA by the microbes was elucidated by determining the presence of ^{13}C -PLFAs. The results indicated the presence of ^{13}C -labeled fatty acids viz. hexadecanoic acid (16:0, Gram-negative bacterial biomarkers), palmitoleic acid (16:1 w7c, Gram-negative bacterial biomarkers), 11-octadecenoic acid (18:1 w7c, Gram-negative and aerobic bacterial biomarkers), linoleic acid (18:2 w6c, Fungal biomarkers) and 13-methyltetradecanoic acid (15:0 iso, Gram-positive bacterial biomarkers) in the natural microcosm spiked with $^{13}C_{12}$ -BPA (Table S10). These results clearly indicate that BPA and/ or its transformation products might be

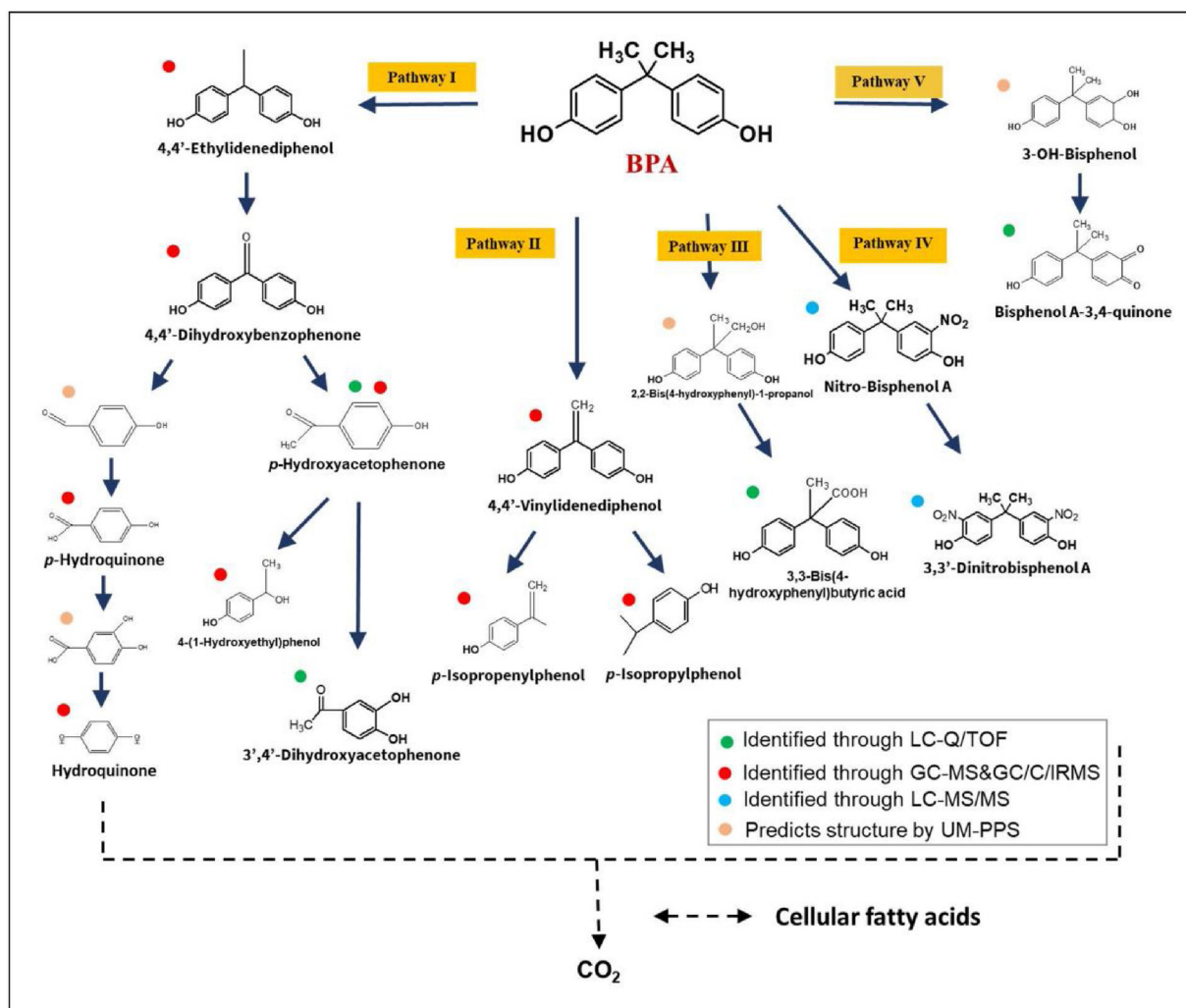


Fig. 4. Proposed pathways of BPA natural attenuation in the surface water.

utilized as a carbon source or via cross-feeding to synthesize cellular membranes by microorganisms in the river water.

3.4. Microbial community characterization

Microbial community diversity was investigated in the microcosm study. Using Miseq sequencing, a total of 197,973 high-quality sequences were generated with an average of $49,493 \pm 9885$ sequences. The sequences were registered in the NCBI sequence read archive database under BioProject numbers PRJNA528530. The microbial community profiles varied at phylum/class (Fig. S6a) and order levels (Fig. S6b). Gammaproteobacteria was the most predominant phylum initially, in the surface water samples. Later an increase in the relative abundance of Cyanobacteria and Alphaproteobacteria in the natural microcosm (Day 7) and microbial degradation microcosm (Day 7) was observed. This was probably due to the lighting effect (Holker et al., 2015) together with the carbon source facilitation as Cyanobacteria was proved for the biological degradation of organic pollutants (Subashchandrabose et al., 2013). The order level abundances showed that Betaproteobacteriales and Frankiales were the predominant orders in the surface water. The relative abundance of Synechococcales increased in the natural attenuation and microbial degradation microcosms at Day 7, while, Rickettsiales increased in the bacterial degradation microcosm at Day 7. The diversity of aquatic microbial communities might be affected by the combination of nutrients and micro-pollutants (Hu et al., 2017). Further studies are needed to

establish a causal relationship between microbial communities and micro-pollutants.

4. Conclusion

Contribution of different biotic and abiotic factors in the attenuation of BPA in natural microcosm was investigated. The SEM approach suggested that microbial degradation involving bacteria was the major factor involved in the natural attenuation of BPA, while, indirect photolysis and other microbes like algae may also play mediatory role in this process. The use of stable carbon isotope tracing and analytical tools viz. GC-MS, GC-C-IRMS and LC-Q/ToF-/MS yielded a total of 14, including 3 novel transformation products that enabled us to propose 5 possible BPA transformation pathways. In some instances, the transformation products were found with higher toxicities than the parent BPA to suggest serious environmental implications of BPA attenuation in the river surface water. Furthermore, the detection of ¹³C-PLFAs indicated the possibility of BPA intrusion in biological systems.

Declaration of competing interests

The authors declare no competing financial interest.

Authors' contributions

YL and QS conceived and designed the study. YL, HZ, KX, HL and

YW performed experimental works. YL, AR, AH, BA and QS evaluated the data, and YL, AR, CY, and QS wrote the manuscript. All authors read and approval to the final manuscript.

Acknowledgements

We appreciated Ms. Xu Liao, Mr. Kun Wu and Miss Lai Wei for the instrument analysis guidance, Ms. Yaying Li and Dr. Jing Ding for the PLFA analysis guidance, Miss. Shuang Li for the microbial analysis guidance. This work was jointly funded by the Natural Science Foundation of Fujian Province (2017J06013), National Science Foundation of China (41573102, 41673099), Youth Innovation Promotion Association CAS(2016280), Joint undergraduates training program of UCAS-XMU, and PIFI CAS (2017VEB0008).

Appendix A. Supplementary data

Supplementary material related to this article can be found, in the online version, at doi:<https://doi.org/10.1016/j.jhazmat.2019.121584>.

References

- Agüera, A., Martínez Bueno, M.J., Fernández-Alba, A.R., 2013. New trends in the analytical determination of emerging contaminants and their transformation products in environmental waters. *Environ. Sci. Pollut. Res. Int.* 20 (6), 3496–3515.
- Barbieri, Y., Massad, W.A., Diaz, D.J., Sanz, J., Amat-Guerri, F., Garcia, N.A., 2008. Photodegradation of bisphenol A and related compounds under natural-like conditions in the presence of riboflavin: kinetics, mechanism and photoproducts. *Chemosphere* 73 (4), 564–571.
- Bletsou, A.A., Jeon, J., Hollender, J., Archontaki, E., Thomaidis, N.S., 2015. Targeted and non-targeted liquid chromatography-mass spectrometric workflows for identification of transformation products of emerging pollutants in the aquatic environment. *Trends Anal. Chem.* 66, 32–44.
- Brenton, A.G., Godfrey, A.R., 2010. Accurate mass measurement: terminology and treatment of data. *J. Am. Soc. Mass Spectrom.* 21 (11), 1821–1835.
- Chen, D., Kannan, K., Tan, H., Zheng, Z., Feng, Y.-L., Wu, Y., Widelka, M., 2016. Bisphenol analogues other than BPA: environmental occurrence, human exposure, and toxicity—a review. *Environ. Sci. Technol.* 50 (11), 5438–5453.
- Chen, L., Xu, Y., Wang, W., Qian, P.-Y., 2015. Degradation kinetics of a potent antifouling agent, butenolide, under various environmental conditions. *Chemosphere* 119, 1075–1083.
- Chin, Y.-P., Miller, P.L., Zeng, L., Cawley, K., Weavers, L.K., 2004. Photosensitized degradation of bisphenol A by dissolved organic matter. *Environ. Sci. Technol.* 38 (22), 5888–5894.
- Ding, Y., Zhou, P., Tang, H., 2016. Visible-light photocatalytic degradation of bisphenol A on NaBiO₃ nanosheets in a wide pH range: a synergistic effect between photocatalytic oxidation and chemical oxidation. *Chem. Eng. J.* 291, 149–160.
- Eio, E.J., Kawai, M., Niwa, C., Ito, M., Yamamoto, S., Toda, T., 2015. Biodegradation of bisphenol A by an algal-bacterial system. *Environ. Sci. Pollut. Res. Int.* 22 (19), 15145–15153.
- Fenner, K., Canonica, S., Wackett, L.P., Elsner, M., 2013. Evaluating pesticide degradation in the environment: blind spots and emerging opportunities. *Science* 341 (6147), 752–758.
- Gao, J., Ellis, L.B.M., Wackett, L.P., 2010. The University of Minnesota Biocatalysis/Biodegradation Database: improving public access. *Nucleic Acids Res.* 38 (Database issue), D488–491.
- Helbling, D.E., Hollender, J., Kohler, Hans-peter E., Singer, Heinz, Fenner, K., 2010. High-throughput identification of microbial transformation products of organic micro-pollutants. *Environ. Sci. Technol.* 44 (17), 6621–6627.
- Hofstetter, T.B., Berg, M., 2011. Assessing transformation processes of organic contaminants by compound-specific stable isotope analysis. *Trends Anal. Chem.* 30 (4), 618–627.
- Holker, F., Wurzbacher, C., Weissenborn, C., Monaghan, M.T., Holzhauser, S.I.J., Premke, K., 2015. Microbial diversity and community respiration in freshwater sediments influenced by artificial light at night. *Philos. Trans. R. Soc. Lond. B Biol. Sci.* 370 (1667).
- Hou, G., Zhang, R., Hao, X., Liu, C., 2017. An exploration of the effect and interaction mechanism of bisphenol A on waste sludge hydrolysis with multi-spectra, isothermal titration microcalorimetry and molecule docking. *J. Hazard. Mater.* 333, 32–41.
- Hu, A., Ju, F., Hou, L., Li, J., Yang, X., Wang, H., Mulla, S.I., Sun, Q., Burgmann, H., Yu, C.-P., 2017. Strong impact of anthropogenic contamination on the co-occurrence patterns of a riverine microbial community. *Environ. Microbiol.* 19 (12), 4993–5509.
- Hu, A., Yang, X., Chen, N., Hou, L., Ma, Y., Yu, C.-P., 2014. Response of bacterial communities to environmental changes in a mesoscale subtropical watershed, Southeast China. *Sci. Total Environ.* 472, 746–756.
- Im, J., Löffler, F.E., 2016. Fate of bisphenol A in terrestrial and aquatic environments. *Environ. Sci. Technol.* 50 (16), 8403–8416.
- Jasper, J.T., Jones, Z.L., Sharp, J.O., Sedlak, D.L., 2014. Biotransformation of trace organic contaminants in open-water unit process treatment wetlands. *Environ. Sci. Technol.* 48 (9), 5136–5144.
- Ji, L., Ji, S., Wang, C., Kepp, K.P., 2018. Molecular mechanism of alternative P450-catalyzed metabolism of environmental phenolic endocrine-disrupting chemicals. *Environ. Sci. Technol.* 52 (7), 4422–4431.
- Ju, L., Wu, P., Yang, Q., Ahmed, Z., Zhu, N., 2018. Synthesis of ZnAlTi-LDO supported C60@AgCl nanoparticles and their photocatalytic activity for photo-degradation of Bisphenol A. *Appl. Catal. B: Environ.* 224, 159–174.
- Kolsek, K., Mavri, J., Sollner Dolenc, M., 2012. Reactivity of bisphenol A-3,4-quinone with DNA. A quantum chemical study. *Toxicol. In Vitro* 26 (1), 102–106.
- Kolvenbach, B., Schlaich, N., Raoui, Z., Prell, J., Zuhlke, S., Schaffer, A., Guengerich, F.P., Corvini, P.F., 2007. Degradation pathway of bisphenol A: does ipso substitution apply to phenols containing a quaternary alpha-carbon structure in the para position? *Appl. Environ. Microbiol.* 73 (15), 4776–4784.
- Li, Y., Rashid, A., Wang, H., Hu, A., Lin, L., Yu, C.-P., Chen, M., Sun, Q., 2018. Contribution of biotic and abiotic factors in the natural attenuation of sulfamethoxazole: a path analysis approach. *Sci. Total Environ.* 633, 1217–1226.
- Limam, I., Limam, R.D., Mezni, M., Guenne, A., Madigou, C., Driss, M.R., Bouchez, T., Mazeas, L., 2016. Penta- and 2,4,6-tri-chlorophenol biodegradation during municipal solid waste anaerobic digestion. *Ecotoxicol. Environ. Saf.* 130, 270–278.
- Liu, Y., Zhang, S., Song, N., Guo, R., Chen, M., Mai, D., Yan, Z., Han, Z., Chen, J., 2017. Occurrence, distribution and sources of bisphenol analogues in a shallow Chinese freshwater lake (Taihu Lake): implications for ecological and human health risk. *Sci. Total Environ.* 599–600, 1090–1098.
- Lobos, J.H., Leib, T.K., Su, T.M., 1992. Biodegradation of bisphenol A and other bisphenols by a gram-negative aerobic bacterium. *Appl. Environ. Microbiol.* 58 (6), 1823–1831.
- Luo, R., Li, M., Wang, C., Zhang, M., Nasir Khan, M.A., Sun, X., Shen, J., Han, W., Wang, L., Li, J., 2019. Singlet oxygen-dominated non-radical oxidation process for efficient degradation of bisphenol A under high salinity condition. *Water Res.* 148, 416–424.
- Ma, C., Qin, D., Sun, Q., Zhang, F., Liu, H., Yu, C.P., 2016. Removal of environmental estrogens by bacterial cell immobilization technique. *Chemosphere* 144, 607–614.
- McCormick, J.M., Van Es, T., Cooper, K.R., White, L.A., Haggblom, M.M., 2011. Microbially mediated O-methylation of bisphenol A results in metabolites with increased toxicity to the developing zebrafish (*Danio rerio*) embryo. *Environ. Sci. Technol.* 45 (15), 6567–6574.
- Molkenthin, M., Olmez-Hanci, T., Jekel, M.R., Arslan-Alaton, I., 2013. Photo-Fenton-like treatment of BPA: effect of UV light source and water matrix on toxicity and transformation products. *Water Res.* 47 (14), 5052–5064.
- Neamtu, M., Frimmel, F.H., 2006. Degradation of endocrine disrupting bisphenol A by 254 nm irradiation in different water matrices and effect on yeast cells. *Water Res.* 40 (20), 3745–3750.
- Peng, Z., Wu, F., Deng, N., 2006. Photodegradation of bisphenol A in simulated lake water containing algae, humic acid and ferric ions. *Environ. Pollut.* 144 (3), 840–846.
- Staples, C., van der Hoeven, N., Clark, K., Mihaich, E., Woelz, J., Hentges, S., 2018. Distributions of concentrations of bisphenol A in North American and European surface waters and sediments determined from 19 years of monitoring data. *Chemosphere* 201, 448–458.
- Subagio, D.P., Srinivasan, M., Lim, M., Lim, T.-T., 2010. Photocatalytic degradation of bisphenol-A by nitrogen-doped TiO₂ hollow sphere in a vis-LED photoreactor. *Appl. Catal. B: Environ.* 95 (3–4), 414–422.
- Subashchandrabose, S.R., Ramakrishnan, B., Megharaj, M., Venkateswarlu, K., Naidu, R., 2013. Mixotrophic cyanobacteria and microalgae as distinctive biological agents for organic pollutant degradation. *Environ. Int.* 51, 59–72.
- Sun, Q., Li, Y., Chou, P.-H., Peng, P.-Y., Yu, C.-P., 2012. Transformation of bisphenol A and alkylphenols by ammonia-oxidizing bacteria through nitrification. *Environ. Sci. Technol.* 46 (8), 4442–4448.
- Sun, Q., Li, Y., Li, M., Ashfaq, M., Lv, M., Wang, H., Hu, A., Yu, C.-P., 2016. PPCPs in Jiulong River estuary (China): spatiotemporal distributions, fate, and their use as chemical markers of wastewater. *Chemosphere* 150, 596–604.
- Tian, Z., Vila, J., Yu, M., Bodnar, W., Aitken, M.D., 2018. Tracing the biotransformation of polycyclic aromatic hydrocarbons in contaminated soil using stable isotope-assisted metabolomics. *Environ. Sci. Technol. Lett.* 5 (2), 103–109.
- Vandenberg, L.N., Hauser, R., Marcus, M., Olea, N., Welshons, W.V., 2007. Human exposure to bisphenol A (BPA). *Reprod. Toxicol.* 24 (2), 139–177.
- Vione, D., Minella, M., Maurino, V., Minerio, C., 2014. Indirect photochemistry in sunlight surface waters: photoinduced production of reactive transient species. *Chemistry* 20 (34), 10590–10606.
- Wang, J., Chapman, S.J., Yao, H., 2016. Incorporation of 13 C-labelled rice rhizodeposition into soil microbial communities under different fertilizer applications. *Appl. Soil Ecol.* 101, 11–19.
- Yamazaki, E., Yamashita, N., Taniyasu, S., Lam, J., Lam, P.K., Moon, H.B., Jeong, Y., Kannan, P., Achyuthan, H., Munuswamy, N., Kannan, K., 2015. Bisphenol A and other bisphenol analogues including BPS and BPF in surface water samples from Japan, China, Korea and India. *Ecotoxicol. Environ. Saf.* 122, 565–572.
- Yan, Z., Liu, Y., Yan, K., Wu, S., Han, Z., Guo, R., Chen, M., Yang, Q., Zhang, S., Chen, J., 2017. Bisphenol analogues in surface water and sediment from the shallow Chinese freshwater lakes: occurrence, distribution, source apportionment, and ecological and human health risk. *Chemosphere* 184 (Suppl. C), 318–328.
- Yang, G., Fan, M., Zhang, G., 2014. Emerging contaminants in surface waters in China—a short review. *Environ. Res. Lett.* 9 (7), 074018.
- Yang, S., Huang, Z., Wu, P., Li, Y., Dong, X., Li, C., Zhu, N., Duan, X., Dionysiou, D.D., 2020. Rapid removal of tetrabromobisphenol A by α -Fe₂O₃-x@Graphene@Montmorillonite catalyst with oxygen vacancies through peroxymonosulfate activation: role of halogen and α -hydroxyalkyl radicals. *Appl. Catal. B: Environ.* 260.
- Yang, S., Wu, P., Liu, J., Chen, M., Ahmed, Z., Zhu, N., 2018. Efficient removal of bisphenol A by superoxide radical and singlet oxygen generated from

- peroxymonosulfate activated with FeO-montmorillonite. *Chem. Eng. J.* 350, 484–495.
- Yu, Y., Han, P., Zhou, L.-J., Li, Z., Wagner, M., Men, Y., 2018. Ammonia monooxygenase-mediated cometabolic biotransformation and hydroxylamine-mediated abiotic transformation of micropollutants in an AOB/NOB coculture. *Environ. Sci. Technol.* 52 (16), 9196–9205.
- Zhang, W., Yin, K., Chen, L., 2013. Bacteria-mediated bisphenol a degradation. *Appl. Microbiol. Biotechnol.* 97 (13), 5681–5689.
- Zhao, X., Qiu, W., Zheng, Y., Xiong, J., Gao, C., Hu, S., 2019. Occurrence, distribution, bioaccumulation, and ecological risk of bisphenol analogues, parabens and their metabolites in the Pearl River Estuary, South China. *Ecotoxicol. Environ. Saf.* 180, 43–52.
- Zielinska, M., Cydzik-Kwiatkowska, A., Bernat, K., Bulkowska, K., Wojnowska-Baryla, I., 2014. Removal of bisphenol A (BPA) in a nitrifying system with immobilized biomass. *Bioresour. Technol.* 171, 305–313.